

RADIATION LOSS AND MECHANICAL HEATING IN THE SOLAR CHROMOSPHERE

PETER ULMSCHNEIDER

Astronomisches Institut der Universität Würzburg, Würzburg, Germany

(Received 6 May, in revised form 24 July, 1974)

Abstract. The radiation loss of the solar chromosphere is evaluated on the basis of the Harvard Smithsonian Reference Atmosphere. The total radiative flux is found to be between 2.5 and 3.3 E6 erg cm⁻² s⁻¹. A discussion of possible heating mechanisms shows that the short period acoustic wave theory is the only one able to balance the chromospheric radiation loss and is consistent with observation.

1. Introduction

In the last few years the accuracy of empirical models of the solar chromosphere has been greatly improved. In the middle and upper chromosphere this was mainly due to the analysis of the Lyman continuum observations of OSO 4 (Noyes and Kalkofen, 1970). For the low chromosphere and the temperature minimum the improved temperature structure was determined by rocket observation at 1650 Å (Parkinson and Reeves, 1969), airborne observations at 300 μ (Eddy *et al.*, 1969) and an H + K line analysis (Linsky and Avrett, 1970). The resulting Harvard Smithsonian Reference Atmosphere (HSRA, Gingerich *et al.*, 1971) may therefore serve as a much more reliable model to estimate chromospheric radiation losses.

Because new calculations are now available for a theoretical radiative equilibrium atmosphere of the Sun (Kurucz, 1974) the chromospheric heating due to purely mechanical means may be inferred with much greater accuracy from the difference between the empirical model, which does include the effect of mechanical dissipation and the theoretical model, which does not include this effect. This calculation restricts severely the conditions which must be met by a chromospheric heating mechanism and allows a much more reliable choice between possible candidates.

In Section 2 we discuss our method of computation of the dominant H⁻ radiation loss and compare it with the method of Praderie and Thomas (1972). Adding the non-LTE Balmer loss we arrive at an approximate total radiation loss (Figure 2 and Tab. I).

In Section 3 we try to balance this radiation loss by various heating mechanisms, arriving at the conclusion that short period acoustic waves are so far the only candidates for a chromospheric heating mechanism. This finding agrees well with similar work done on older empirical models (Ulmschneider, 1970).

2. Radiative Losses

2.1. DISCUSSION OF THE PRADERIE AND THOMAS RADIATION LOSS

In the low chromosphere radiative losses are mainly due to the H⁻ ion and the Balmer

series of hydrogen (Athay, 1966). There exists however some discrepancy how to compute this radiative loss (Osterbrock, 1961; Athay, 1966, 1970; Ulmschneider, 1970; Praderie and Thomas, 1972). Praderie and Thomas recently discussed the difference between the computations of Athay and Osterbrock. They found that they agree with Osterbrock but that Athay's value is incorrect and too low by a factor of 2. However, their value is still lower by a factor of 2 relative to Ulmschneider's result. In order to show how this additional factor of 2 arises we recompute the case used by Praderie and Thomas.

Praderie and Thomas (1972) compute the change in flux $\Delta\pi F$ produced by an atmosphere which is perturbed out of radiative equilibrium (RE) by a constant jump ΔB in the source function for optical depths less than τ_c . τ_c is small and in the solar atmosphere typically 10^{-4} . We have

$$\Delta\pi F = \pi F_{\text{non-RE}} - \pi F_{\text{RE}} = \int_{\infty}^0 \frac{d\pi F}{d\tau} d\tau. \quad (1)$$

Introducing the mean intensities J , J_0 and source function B , B_0 of the non-RE and RE atmospheres respectively we have

$$\Delta\pi F = 4\pi \int_{\infty}^0 (J - B - J_0 + B_0) d\tau, \quad (2)$$

where

$$\begin{aligned} B &= B_0 + \Delta B & \text{for } \tau \leq \tau_c, \\ B &= B_0 & \text{for } \tau > \tau_c. \end{aligned} \quad (3)$$

Evaluating J with help of the transfer equation we get

$$\Delta\pi F = \Delta\pi F_1 + \Delta\pi F_2, \quad (4)$$

where

$$\begin{aligned} \Delta\pi F_1 &= 4\pi \int_{\tau_c}^0 (J - J_0 - \Delta B) d\tau = \\ &= -2\pi\Delta B \left\{ \int_0^1 d\mu \mu (1 - e^{-\tau_c/\mu}) - \int_{-1}^0 d\mu \mu (1 - e^{\tau_c/\mu}) \right\}, \end{aligned} \quad (5)$$

and

$$\Delta\pi F_2 = 4\pi \int_{\infty}^{\tau_c} (J - J_0) d\tau = 2\pi\Delta B \int_{-1}^0 d\mu \mu (e^{\tau_c/\mu} - 1). \quad (6)$$

Because τ_c is very small we may expand the exponential functions in Equations (5) and (6) around 0 and obtain to first order

$$\Delta\pi F_1 = 4\pi\Delta B\tau_c \quad (7)$$

and

$$\Delta\pi F_2 = -2\pi\Delta B\tau_c. \quad (8)$$

Inserting these results into Equation (4) we obtain the same total flux $\Delta\pi F = 2\pi\Delta B\tau_c$ as Praderie and Thomas (1972). However, this is not the flux relevant for the computation of the nonradiative energy input of the solar chromosphere. The relevant flux is actually $\Delta\pi F_1$ and is larger by a factor of 2 compared with $\Delta\pi F$.

To understand this we assume the simplified picture of a mechanical wave travelling adiabatically towards lower optical depth. Because of the formation of shocks at the height of the temperature minimum the wave starts to dissipate mechanical energy and produces the source function jump ΔB . In the optically thin region this results in a loss of photons in all direction. This loss which goes in both inward and outward directions is the one which balances the mechanical dissipation. Naturally because the inward going photons are reabsorbed, the total flux $\Delta\pi F$ is only $\frac{1}{2}\Delta\pi F_1$. However it is $\Delta\pi F_1$ which balances mechanical dissipation.

This result is obvious if one considers the chromosphere to be an isolated optically thin slab of thickness τ_c . Taking $B_0 = J_0 = 0$ in Equation (2) we have for small τ_c

$$F(\tau) \approx 2\pi\Delta B(\tau_c - 2\tau). \quad (9)$$

Thus we find

$$\Delta\pi F = \pi F(0) - \pi F(\tau_c) = \Delta\pi F_1 = 4\pi\Delta B\tau_c. \quad (10)$$

The mechanical dissipation therefore leads to the flux $\Delta\pi F_1$.

In order to show that this result agrees with the formula of Ulmschneider (1970) we consider $J - J_0$ in Equation (5). We find

$$J - J_0 \approx \frac{1}{2}\Delta B\tau_c \quad (11)$$

which because of small τ_c may be neglected relative to ΔB in Equation (5). Thus we have for the relevant radiative flux

$$\Delta\pi F_1 = -4\pi \int_{\tau_c}^0 \Delta B \, d\tau \quad (12)$$

or equivalently the simple formula

$$\frac{d\pi F_1}{dh} = 4\pi \int_0^\infty K_\nu (B_\nu(T) - B_\nu(T_0)) \, d\nu, \quad (13)$$

which was used by Ulmschneider (1970).

2.2. CHROMOSPHERIC RADIATION LOSS

In the computation of the chromospheric radiation loss which is balanced by mechanical heating we must specify both the empirical temperature structure T and the temperature profile T_0 which would be there if no mechanical heating were present. Kurucz (1974) has computed such a theoretical radiative equilibrium temperature

profile T_0 . The main feature of this profile is an almost linear decrease of temperature versus the logarithm of the optical depth near the observed temperature minimum. However Kurucz finds for $\tau_{5000} < 1.0 \text{ E} - 3$ a temperature, larger by about 150 K than the observed temperature profile of the HSRA. As the effect of radiative damping on hydrodynamic waves emanating out of the Sun is to overestimate the observed temperature profile relative to the radiative equilibrium atmosphere (Ulmschneider and Kalkofen, 1973) we would expect that the theoretical profile stays below the observed one. This indicates that either the HSRA seems to be too low by about 200 K around the temperature minimum or that the theoretical atmosphere is too high by the same amount.

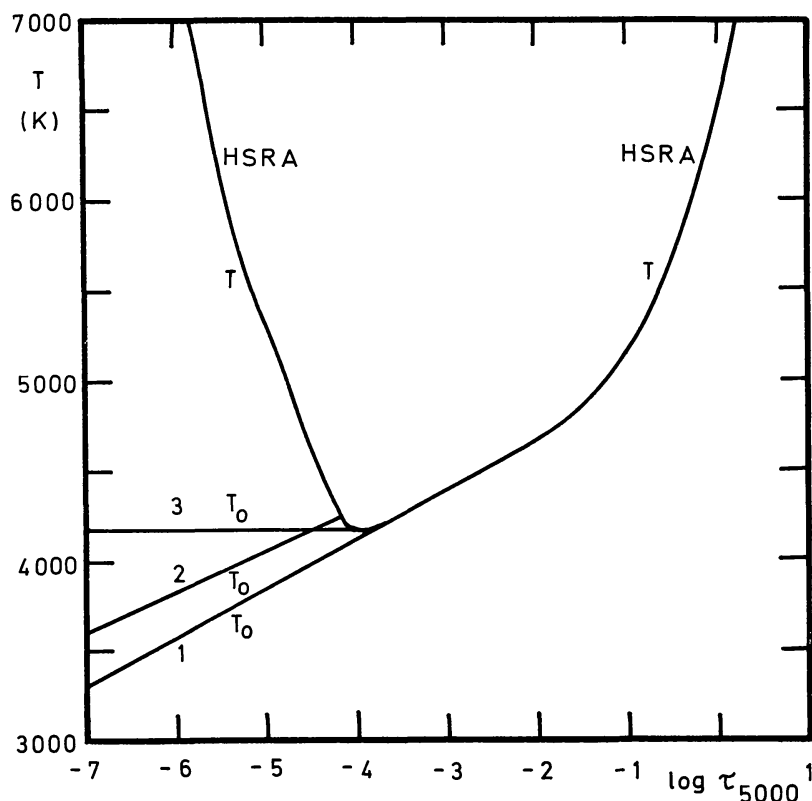


Fig. 1. Temperature vs. optical depth distribution for the empirical models (T , HSRA) which include, and the theoretical models (T_0 , cases 1-3) which do not include mechanical heating.

Because of this uncertainty we have computed various cases as indicated in Figure 1. The HSRA is used in all cases as the empirical temperature distribution T . In case 1 we choose for the radiative equilibrium model the distribution

$$T_0 = 4250 + 260(\log \tau_{5000} + 3.5) \text{ K.} \quad (14)$$

For case 2 we simply use the Kurucz (1974) model for optical depths less than $\tau_{5000} = 1.0 \text{ E} - 4$.

Finally for case 3 we take the radiative equilibrium model as being simply constant, $T_0 = 4170 \text{ K}$ for optical depths less than the temperature minimum.

The radiation loss/due to H^- is now computed integrating Equation (13) with 40 frequency points up to the Lyman limit using the H^- opacity routine given by Ginge- rich (1964). The Balmer loss was evaluated following Athay (1966)

$$\left. \frac{d\pi F}{dh} \right|_{\text{Ba}} = N_2 C_{23} \langle hv_{u2} \rangle, \quad (15)$$

where $\langle hv_{u2} \rangle = 4.0 \text{ E} - 12$ is a mean energy for the Balmer series (Ulmschneider, 1970). For the collisional excitation rate C_{23} we use a formula given by Peterson (1969, p. 33) based on the BOW cross sections (Burke *et al.*, 1967). N_2 was computed taking $b_2 = b_1$ under the assumption of detailed balance in the $L\alpha$ line (see Noyes and Kalkofen, 1970).

The resulting chromospheric radiative loss rate as function of height is shown in Figure 2. We see that the uncertainty in the knowledge of the radiative equilibrium temperature distribution T_0 relative to the empirical distribution T influences the radiative loss rate very little. This makes it highly unlikely that the Cayrel mechanism will alter this result significantly (cf. Athay, 1970). The total computed radiative flux

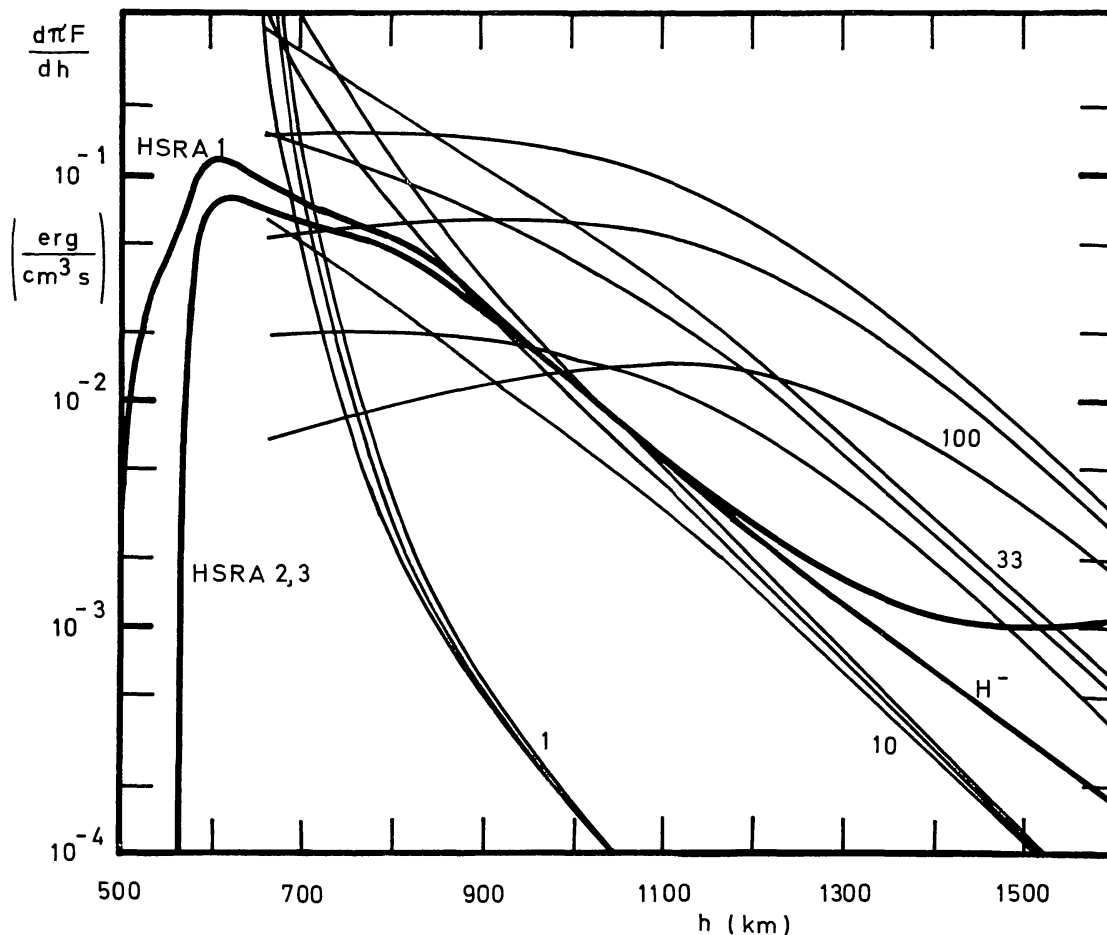


Fig. 2. Radiation loss rates (heavy lines) compared with shock dissipation rates (thin lines) in the HSRA, assuming different theoretical model cases 1–3. H^- labels the H^- contribution. The shock dissipation curve families are labeled by the wave periods in seconds and have initial fluxes $1.0 \text{ E}6$, $4.0 \text{ E}6$, $8.0 \text{ E}6 \text{ erg cm}^{-2} \text{ s}^{-1}$, bottom to top.

$\Delta\pi F_1$ of the chromosphere is given in the first column of Table I. Adding the observed $2.0 \text{ E5 erg cm}^{-2} \text{ s}^{-1}$ for $L\alpha$, plus an equal amount of flux for the H + K lines and other neglected emitters the total radiative flux of the chromosphere is given in the second column of Table I. The Ba emission flux up to 1600 km amounts to about $4.0 \text{ E4 erg cm}^{-2} \text{ s}^{-1}$. Table I shows also recent computed chromospheric fluxes reported in the literature.

TABLE I

Total computed H^- plus Ba flux $\Delta\pi F_1$ and, adding observed XUV fluxes, the total chromospheric radiation flux $\Delta\pi F_c$ in $\text{erg cm}^{-2} \text{ s}^{-1}$ for various assumptions as to the T and T_0 temperature distributions (cases 1–3). Recent values of $\Delta\pi F_1$ given in the literature are also shown.

$\Delta\pi F_1 \text{ erg cm}^{-2} \text{ s}^{-1}$	$\Delta\pi F_c \text{ erg cm}^{-2} \text{ s}^{-1}$	
5.6 E6		Athay (1966)
2.0 E6		Athay (1970)
2.2 E6		Ulmschneider (1970)
2.9 E6	3.3 E6	case 1
2.1 E6	2.5 E6	case 2
2.1 E6	2.5 E6	case 3

3. The Heating Mechanisms

We have to ask which mechanisms provide a total mechanical flux equal to $\Delta\pi F_c$ and are able to balance the computed radiation loss $d\pi F_c/dh$ at every height. In the following we check a list of candidates.

3.1. POSSIBLE HEATING MECHANISMS

3.1.1. 300 s Oscillations

There are two reasons against their relevance as a heating agent of the chromosphere. These oscillations exhibit (Evans *et al.*, 1963) a 90° phase shift between the temperature and velocity oscillation which resembles a standing wave with no appreciable energy transport. Canfield and Musman (1973) have observed an energy flux of $8.0 \text{ E5 erg cm}^{-2} \text{ s}^{-1}$ at 490 km and of $2.0 \text{ E4 erg cm}^{-2} \text{ s}^{-1}$ at 1000 km in the HSRA. This is between a factor of 4 and one order of magnitude below the flux $\Delta\pi F_c$ needed.

3.1.2. Running Penumbra Waves

Zirin and Stein (1972) observed running penumbral waves with an energy flux of about $50 \text{ erg cm}^{-2} \text{ s}^{-1}$. Here again the necessary energy requirement is not met in order to serve as a candidate for chromospheric heating.

3.1.3. Magnetohydrodynamic Waves

These waves, especially Alfvén waves, are very likely candidates for the heating above sunspots for the high chromosphere and the corona above supergranulation boundaries

producing the K line network (cf. Uchida and Kaburaki, 1974). However because of the low energy density of the magnetic field away from sunspots, being typically four orders of magnitude less than the energy density of the gas near the temperature minimum, a purely gas-dynamic mechanism is much more probable to produce the required heating of the low chromosphere.

That in the low chromosphere away from sunspots the heating mechanism is non-magnetic is moreover suggested by the appearance of spectroheliographic images of the solar disk (e.g. Reeves and Parkinson, 1970). The solar image in lines originating in the lower and middle chromosphere below and up to the level of formation of the Lyman continuum appears uniform while in the XUV lines of the transition region the solar image strongly shows the network structure. In these lines the emission is highly correlated with regions of strong magnetic field. This disparity between chromospheric and transition region spectroheliograms is also seen in recent observations of much higher resolution (Vernazza, 1974).

3.1.4. *Internal Gravity Waves*

These waves (Whitaker, 1963) have several disadvantages as candidates for chromospheric heating. They propagate generally horizontally and have a low frequency. Because of this, gravity waves should have – but have not – been observed so far. In addition radiative damping severely affects gravity waves (Stix, 1970; Souffrin, 1972). It is doubtful whether they cross at all the zone of strong radiative damping around $\tau=0.1$ to 1.0 although they are produced efficiently (Stein, 1966, 1967).

3.1.5. *Acoustic Waves*

These waves already proposed as heating agents of the chromosphere by Biermann (1946) and Schatzmann (1949) seem to be the only serious candidates for the heating mechanism of the low chromosphere.

3.2. THE SHORT PERIOD ACOUSTIC HEATING MECHANISM

We have essentially three points in favor of the theory that short period acoustic waves can in fact provide the necessary heating of the low chromosphere.

3.2.1. *Total Energy Generation*

Stein (1968) has computed the energy flux spectrum of acoustic waves produced in the convection zone of the Sun. The total acoustic energy is 2 orders of magnitude larger than the amount needed for the heating of the chromosphere. However as Ulmschneider (1971b) has shown, this energy excess is spent by radiative damping in the upper photosphere, when the wave penetrates this region. A detailed computation of the effect of radiative damping is missing at the moment, but will be available shortly (Ulmschneider and Kalkofen, 1974).

3.2.2. *Energy Dissipation Rate*

Stein (1968) has shown that the acoustic energy emanates in form of a spectrum with a

maximum around the periods 29–38 s and a range of periods from about 5 to 300 s. If, for simplicity, we assume that this acoustic energy appears as one monochromatic wave which after the temperature minimum is transformed into a sawtooth shock wave, we may use the weak shock theory to evaluate the dissipation as function of height in the solar atmosphere. This is done, keeping the initial energy input and the period of the wave as free parameters. The shock equation in the weak shock theory reads (Ulmschneider, 1970):

$$\frac{d\bar{\eta}}{dh} = \frac{\bar{\eta}}{2} \left(\frac{\gamma g}{c^2} - \frac{3}{2c^2} \frac{dc^2}{dh} - \frac{(\gamma + 1)\bar{\eta}v}{c} \right), \quad (16)$$

where $\bar{\eta}$ is the strength of the shock.

The mechanical flux is given by

$$\pi F_{\text{mech}} = \frac{1}{12} \gamma p c \bar{\eta}^2, \quad (17)$$

the dissipation rate by

$$\frac{d\pi F_{\text{Mech}}}{dh} = -\frac{1}{12} \gamma (\gamma + 1) p \bar{\eta}^3 v. \quad (18)$$

In Figure 2 we show the resulting dissipation rates vs. height of waves having periods of 1, 10, 33 and 100 s and fluxes of 1.0 E6, 4.0 E6 and 8.0 E6. It is seen that a short period shock wave with $P \approx 10\text{--}20$ s is well able to balance the chromospheric radiation loss at every height. Waves of very much larger and smaller periods are excluded because they have very different dissipation behavior. Moreover the optimal period of 10–20 s agrees well with the maximum period found in the spectrum computations of Stein (1968), allowing for the fact that shorter period waves will transform into shock waves earlier (Ulmschneider, 1971a).

The weak shock theory has recently come under attack by Stein and Schwartz (1973) who compared the theory with their fully nonlinear computations. They found that the weak shock theory gives too much dissipation especially for large wave periods. The agreement between the weak shock theory and the nonlinear calculations is, however, good for small periods of less than 50 s. While some of the discrepancy between the two theories may be attributed to the way in which the parameters of the weak shock theory, such as the shape of the sawtooth profile or the initial height in the atmosphere, are chosen, the fact that long period waves show less dissipation in the nonlinear theory actually strengthens our argument.

If the 100 sec waves of Figure 2 dissipate less energy than indicated, more energy will be conserved and cause a much stronger growth of the wave. This will result in a much stronger increase of the

$$\left. \frac{d\pi F}{dh} \right|_{\text{Mech}}$$

versus height curve and a lowering of the point where the shock wave is introduced. This is contrary to the behavior of the radiative loss curve which decreases with height.

3.2.3. Observations

As we have seen in the beginning of this section the observations so far were unable to identify a mechanical phenomenon of sufficient energy to explain the chromospheric heating. However mechanical heating plays an important role in the chromosphere as shown by Boland *et al.* (1973) who observed that strong microturbulence occurs in XUV lines.

Thus we might be faced with the fact that the actual mechanism is in principle unobservable. For a wave with a 20 s period we have in the chromosphere a wavelength of 140 km which is smaller than the line-contributing region of any chromospheric line. Thus a wave of this period can not be detected by periodic frequency displacements. It must be detected by the microturbulence which it produces. Oster and Ulmschneider (1973) have shown that the resulting microturbulence is only large if the velocity amplitude is close to the sound velocity. This is however not the case here. A wave with the energy flux needed for solar chromosphere has at the temperature minimum because of

$$\rho v^2 c = 3.0 \text{ E6 erg cm}^{-2} \text{ s}^{-1}, \quad (19)$$

an amplitude of $v = 3.8 \text{ E4 cm s}^{-1}$ or 5% of the sound velocity. Therefore the small amplitude waves involved in the heating of the low chromosphere are difficult to detect through their microturbulence.

4. Conclusion

A recomputation of the chromospheric radiation loss on basis of the HSRA shows that the small period acoustic heating theory of the chromosphere is presently the sole mechanism which is able to explain the energy balance in the low chromosphere.

References

- Athay, R. G.: 1966, *Astrophys. J.* **146**, 223.
 Athay, R. G.: 1970, *Astrophys. J.* **161**, 713.
 Biermann, L.: 1946, *Naturwissenschaften* **33**, 118.
 Boland, B. C., Engstrom, S. F. T., Jones, B. B., and Wilson, R.: 1973, *Astron. Astrophys.* **22**, 161.
 Burke, P. G., Ormonde, S., and Whitacker, W.: 1967, *Proc. Phys. Soc.* **92**, 319.
 Canfield, R. C. and Musman, S.: 1973, *Astrophys. J.* **184**, L131.
 Eddy, J. A., Léna, P. J., and MacQueen, R. M.: 1969, *Solar Phys.* **10**, 330.
 Evans, J. W., Michard, R., and Servajean, R.: 1963, *Ann. Astrophys.* **26**, 368.
 Gingerich, O.: 1964, *SAO Spec. Report* **167**, 19.
 Gingerich, G.: Noyes, R. W., Kalkofen, W., and Cuny, Y.: 1971, *Solar Phys.* **18**, 347.
 Kurucz, R. L.: 1974, *Solar Phys.* **34**, 17.
 Linsky, J. and Avrett, E. H.: 1970, *Publ. Astron. Soc. Pacific* **82**, 169.
 Noyes, R. W. and Kalkofen, W.: 1970, *Solar Phys.* **15**, 120.
 Oster, L. and Ulmschneider, P.: 1973, *Astron. Astrophys.* **29**, 1.
 Osterbrock, D. E.: 1961, *Astrophys. J.* **134**, 347.
 Parkinson, W. H. and Reeves, E. M.: 1969, *Solar Phys.* **10**, 342.
 Peterson, D. M.: 1969, *SAO Spec. Report* **293**, 33.

- Praderie, F. and Thomas, R. N.: 1972, *Astrophys. J.* **172**, 485.
Reeves, E. M. and Parkinson, W. H.: 1970, *Astrophys. J. Suppl.* **21**, 1.
Schatzman, E.: 1949, *Ann. Astrophys.* **12**, 203.
Souffrin, P.: 1972, *Astron. Astrophys.* **17**, 458.
Stein, R. F.: 1966, Ph.D. Thesis, Columbia University, New York.
Stein, R. F.: 1967, *Solar Phys.* **2**, 385.
Stein, R. F.: 1968, *Astrophys. J.* **154**, 297.
Stein, R. F. and Schwartz, R. A.: 1973, *Astrophys. J.* **186**, 1083.
Stix, M.: 1970, *Astron. Astrophys.* **4**, 189.
Uchida, Y. and Kaburaki, O.: 1974, *Solar Phys.* **35**, 451.
Ulmschneider, P.: 1970, *Solar Phys.* **12**, 403.
Ulmschneider, P.: 1971a, *Astron. Astrophys.* **12**, 297.
Ulmschneider, P.: 1971b, *Astron. Astrophys.* **14**, 275.
Ulmschneider, P. and Kalkofen, W.: 1973, *Solar Phys.* **28**, 3.
Ulmschneider, P. and Kalkofen, W.: 1974, to be published.
Vernazza, J.: 1974, private communication.
Whitaker, W. A.: 1963, *Astrophys. J.* **137**, 914.
Zirin, H. and Stein, A.: 1972, *Astrophys. J.* **178**, L85.